23rd International Conference on Renewable Energies and Power Quality (ICREPQ'25)
Tenerife (Spain), 25th to 27th June 2025
Renewable Energy and Power Quality Journal (RE&PQJ)
ISSN 2172-038 X, Volume No.23, September 2025

Bifacial Photovoltaics for DC Fast Public Charging of 800V Electric Vehicles

G. S. Quansah[1], O. Oñederra[1], G. Saldaña[1], M. González-Pérez[2] and I. Zamora[1]*.
[1]Department of Electrical Engineering, Engineering School of Bilbao, University of the Basque Country, Bilbao, Spain
[2]Department of Electrical Engineering, Engineering School of Gipuzkoa, University of the Basque Country, Eibar, Spain
*Correspondence: inmaculada.zamora@ehu.eus

Abstract. Electric Vehicles (EVs) operating on 800V architecture, and their associated fast-charging stations, demand higher power capacity, as compared to traditional 400V EVs. This increases stress on the utility grid. Bifacial photovoltaics (bPVs) offer a high-performance energy generation solution, capable of mitigating these demands. They are known for their bidirectional irradiance capture technology, and dual-surface PV conversion capability. Using superior photon-to-electron conversion efficiencies and enhanced power density, bPVs show an advantage over monofacial photovoltaics (mPVs). This paper evaluates the energy generation potential of bPVs, integrated with grid-supplied power, to support 800V EV charging requirements. This is achieved through computational modeling and simulation with PVSyst, using meteorological datasets, from selected regions in Spain. For space-constrained urban areas, this paper technically validates that energy output of bPVs represent a superior strategy for supporting the electrical grid, in the charging of 800V EVs, as compared to traditional mPVs.

Key words. Bifacial, Albedo, DC Fast Charging, 800V, Electric Vehicle

Acronyms – PV(Photovoltaic), bPV(bifacial PV), mPV (monofacial PV), P.R (Performance Ratio), C.F. (Capacity Factor), DCFCS (Direct Current Fast Charging Station), CS (Charging Station), CP (Charging Port), CE (Charging Event), GCR (Ground Coverage Ratio), BF (Bifaciality Factor), DoD (Depth of Discharge)

1. Introduction

Automobile manufacturers, in recent years, are increasingly upgrading EV powertrain architectures from 400V to 800V systems, to enhance overall performance. The terms '400V' and '800V' refer to nominal voltage ranges rather than fixed magnitudes. In 400V systems, the nominal operating range typically spans from 300V to 500V, whereas 800V systems function within a range of 600V to 900V. The transition to an 800V architecture involves a total redesign of the EV's electrical system, including critical subsystems, such as power inverters, electric traction motors, high-voltage energy distribution networks, and the charging interface. Increasing the vehicle's internal operating voltage impacts not only its internal high-voltage components, but also its interoperability and compliance with external public infrastructure [1]. The adoption of an 800V EV architecture achieves superior charging efficiency, by reducing current demand during high-power transfer. This minimizes the Joule heating losses. Another advantage of switching to 800V EVs is that, because of reduced current density requirements, there is a decrease in the cross-sectional area of power conductors, located within the vehicle's wiring and high-voltage circuits. This enables the use of lower-gauge cables and smaller passive components [2]. However, the deployment of 800V EV architectures requires high-power charging stations capable of facilitating energy transfer rates, approaching or exceeding 350kW. Direct Current Fast Charging Stations (DCFCSs), specifically engineered for 800V systems, are critical for meeting these requirements [3]. The higher power demands of this 800V EV-compatible charging stations would require careful integration with renewable energy sources (RES). RES, such as PV systems, when optimally integrated with 800V-compatible charging stations, can mitigate grid congestion and reduce grid dependency. The operational efficiency of PV systems is governed by parameters such as solar irradiance, which typically ranges from 3 to 7kWh/m²/day [4]. Other parameters include geographical location, seasonal variations, and the angle of solar incidence. In recent years, arrays of mPVs, supplemented by utility grid interconnection, have been delivering power to EV charging stations, to meet demand profiles [4]. However, the demand for high-power charging systems for 800V EVs, which require up to 350kW of power, often exceeds the functional limitations of mPVs. Hence, the adoption of bPVs, to provide the extra power. This paper conducts this research and further derives the optimal tilt angle for maximizing energy capture from bPV arrays. The analysis features site-specific solar irradiance profiles, and seasonal variability in incident radiation, to optimize the energy output across selected Spanish cities. It also evaluates the effects of pitch, limiting angle, and ground coverage ratio (GCR), on PV system energy output. The paper begins by giving a brief description of the need to integrate DCFCS with bPVs for 800V EV Charging. The methodology follows, using the PVSyst software tool, for modelling and simulations. The results are obtained, comparing energy outputs of bPVs and mPVs,

respectively, and ends with the conclusion, and future recommendations suggested.

2. DC Fast Charging Stations integration with bPVs for 800V Electric Vehicles

In space-constrained urban environments, bPVs achieve increased energy generation compared to mPVs for equivalent surface areas. This makes them ideal for meeting the high-power demands of DCFCSs, which support 800V EV architectures.

2.1 800V Electric Vehicles

While the voltage range of the 800V system doubles from the 400V system, the overall energy capacity of the battery pack and the total cell count remain unchanged. This is achieved with an optimized battery configuration. The 400V system uses a 100 series by 4 parallel (100s4p) arrangement, delivering 300V to 420V. In the 800V system, this shifts to a 200 series by 2 parallel (200s2p) design, delivering 600V to 840V [2].The 2 cells connected in parallel, each rated with a maximum charge current of 150A, combine to achieve a maximum total charge current of 300A. Consequently, the maximum charging power of the system reaches approximately 249kW. This enhanced power level allows for faster charging by DCFCSs, reducing the charging time by 25% [2].

2.2 DC Fast Charging Stations

DCFCSs are vital in providing rapid charging for EVs, especially those using 800V systems. Off-board chargers, located externally, deliver higher power levels directly to the vehicle's battery, enabling faster charging. In contrast, on-board chargers, integrated within 800V EVs, are employed when external high-voltage infrastructure like DCFCS, is limited or unavailable. These on-board chargers are constrained by EV power limitations, resulting in slower charging rates than the, more powerful off-board chargers used for DCFCS [3]. While AC Chargers are common for residential and lower-power applications, DC Chargers are mostly the preferred choice for rapid charging at public stations, due to their higher power output [5]. DCFCSs can be connected to an AC or DC network or microgrid. In AC-connected fast charging stations, each individual charger is equipped with its own DC-DC conversion stage, to transform the AC power from the grid into the DC power required by the EV's battery. In DC-connected fast charging stations, the conversion of AC power from the grid to DC power occurs at a central point through a single rectification stage (an AC-to-DC converter). Once converted, the DC power is distributed directly to the individual chargers, saving costs and improving efficiency [6]. Some notable examples of DC-connected DCFCSs include Tritium PKM150, with efficiency above 97%, Tritium NEVI System, and the Enercon E-charger 600, with efficiency greater than 94% [9]. These and other similar DCFCSs have power outputs ranging from 22-150kW. Emerging ones have their range from 200-350kW, ideal for 800V EVs. Widely adopted global DC charging standards include CHAdeMO, the Combined Charging System (CCS), and the Tesla Supercharger [5]. To meet the high-power demands of DCFCSs during peak loads, bPVs play an integral role through dual-surface energy harvesting.

2.3 Bifacial Photovoltaics

The modules of bPVs are designed to capture solar radiation from their front and back sides, unlike traditional mPVs [7]. In high irradiance regions, mPVs typically achieve energy outputs of 1,600–1,900kWh/kWp every year, receiving 5–7 kWh/m²/day. In comparison, bPVs exhibit superior performance, with energy outputs, rising to 1,800–2,300kWh/kWp every year. The albedo effect influences rear-side energy gains in bPVs. High-albedo surfaces, such as snow offers 80% reflectivity, concrete around 25-35% (as used in this paper), sand around 30–40%, and vegetation, from 20–25%, contributing to rear-side energy gains of 10–30% [8]. Similarly, the choice of PV cell technology, also affects energy output. The performance metrics of PV systems are intrinsically linked to the material properties and structural characteristics of the active semiconductor layers. Monocrystalline silicon cells, characterized by near-perfect crystalline lattice alignment, high minority carrier diffusion lengths, reduced bulk recombination rates, and low series resistance, are normally used for mPV and bPV module manufacture. In bPV configurations, these cells achieve efficiencies of 21–24%, due to their enhanced rear-side albedo absorption and bifacial photon harvesting capabilities. This is in comparison to 20–22% for mPVs. Conversely, polycrystalline silicon cells are limited by high-density grain boundary states, increased intragranular scattering, lower carrier collection probability, and suboptimal short-circuit current density. The polycrystalline silicon cells, due to these limitations, achieve efficiencies of only 15–17%, making them less suitable for advanced bPV systems, which require high energy-conversion ratios under variable angular irradiance distributions [7]. Another key phenomenon which affects PVs is peak shaving, a strategy used to reduce the instantaneous load on the power grid, during periods of high demand. By reducing peak loads, peak shaving enhances the stability of the grid and improve power quality. DCFCSs, integrated with bPV panels, can play a key role, by shifting their charging rates to match off-peak periods, reducing their impact on the grid during peak times [9]. `

3. Methodology

The methodology developed in this paper involves modeling the integration of DCFCSs with bPVs, to meet the high-energy demand profiles of 800V EV charging. A combination

of simulation and data analysis is employed to evaluate energy output, and system efficiency in urban environments with limited space.

3.1 Site Selection and Climate Profile

Solar irradiance datasets, including Global Horizontal Irradiance (GHI), Direct Normal Irradiance (DNI), and Diffuse Horizontal Irradiance (DHI), are sourced from Spain's Agencia Estatal de Meteorología (AEMET), NASA's solar resource data, and the National Solar Radiation Database (NSRDB). These solar irradiance datasets form the basis for evaluating the energy output of bPVs, under different atmospheric conditions, across seven Spanish cities: Barcelona (BNA), Madrid (MAD), Bilbao (BIL), Zaragoza (ZGZ), Tenerife (TFE), Seville (SEV), and Almeria (ALM). The GHI profiles of these locations are depicted in Figure 1. Energy output computations are done, using the PVSyst simulation tool, which employs irradiance-dependent performance models and storage system integration analysis. The load profiles of DCFCS are evaluated, and bPVs simulated. This is to satisfy the dynamic power requirements, under variable irradiance and operational constraints.

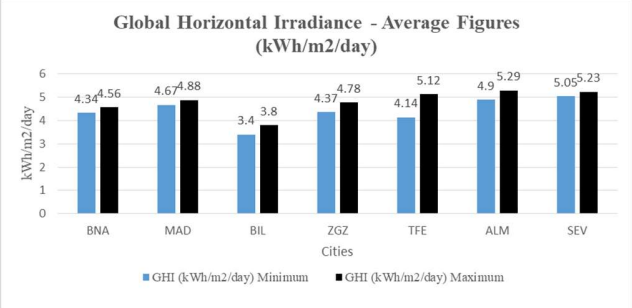

Figure 1. GHI for selected Spanish Cities [10].

3.2 Energy Profile of 800V EV DC Fast Charging Stations

The energy profile of 800V EV DCFCSs depends on power levels, usage, and charging events. The following characteristics must be considered:

- DCFCSs for 800V EVs operate at power levels ranging from 50kW to 350kW or higher.
- How busy a charging station is, determines the energy needs, and efficiency. Every charging station (CS) has a number of individual charging ports (CP). Low-usage CSs typically have 2 CPs, and a peak power demand of 150kW. In contrast, a high-usage CS has 6 ports, with a higher peak power demand of up to 474kW [11].
- A charging event (CE) refers to a single EV accessing a charging port for recharging. The number of CE per CP each day depends on usage, with low-usage having 2 CE and high-usage having 16 CE for an EV [11].
- Each CE for 800V EVs takes 30 minutes or less to charge the battery, from 10% to 80%. [6]. Since most DCFCS are located in cities, it is likely they will have high-usage, with about 16 CE per CP each day.
- The daily total estimated energy demand for a high-usage DCFCS is therefore computed, as shown in Table 1, and given by equation (1).

$$T_D = P_o \text{ *(No. of CP) *(No. of CE/CP) *(No. of hrs/CE) ……. (1)}$$

Table 1. Daily Energy Demand for High-Usage DCFCS

Output Power, Po (kW)	*No. of CP*	*No. of CE/CP*	*No. of hrs/CE*
350	6	16	0.5
T_D = 16800kWh = 16.800MWh			

- For the 6-port charging station, equipped with 350kW DCFCS, the total estimated daily energy demand is calculated as 16800kWh/day (16.80MWh/day). This energy requirement serves as the basis for PV system modeling to ensure adequate energy generation and supply.

3.3 Energy Output – Photovoltaic Modelling

PV modelling has been carried out using the PVSyst software tool to model the performance characteristics of bPVs and mPVs. High-efficiency PV modules are sourced from Longi Solar, a manufacturer recognized for advanced bifacial technology. To ensure methodological consistency, and eliminate variances in module-specific electrical parameters, including I-V curve characteristics, fill factor and thermal performance, both bPV and mPV arrays, are selected from the same manufacturer.

Table 2. Comparison of mPV and bPV Module Specifications

Specification	Monofacial (LR5-72HPH-545M)	Bifacial (LR5-72HBD-545M)
Peak Power Output, P_{peak} (W)	546.1	546.1
Panel Wattage, P_{panel} (Wp)	545	545
Maximum Power Point Voltage, V_{MPP} (V)	41.80	41.80
Maximum Power Point Current, I_{MPP} (A)	13.040	13.040
Open Circuit Voltage, V_{OC} (V)	50.30	50.30
Short Circuit Current, I_{SC} (A)	13.920	13.920
Bifaciality Factor, BF	Not applicable	0.8
Albedo (Concrete surfaces), α	Not applicable	0.35

This enables a controlled comparative performance assessment as seen in Table 2. In this research, a distributed topology is employed for the PV array system, which features

a module efficiency of 23.55%. The system consists of 1,098 PV modules configured into 61 parallel strings, with 18 modules connected in series per string. Each module has a cross-sectional area of 2.56m², collectively spanning a total cross-sectional area of 2814m². The modules are further distributed across the concrete rooftops of multiple adjacent buildings. The European Solar Rooftops Initiative requires rooftop solar systems on all new public and commercial buildings, with roofs larger than 250 m² by 2026, on existing ones by 2027, and on all new residential buildings by 2029 [12]. In alignment with this directive, the PV system, with a total deployment area of 2814m², could be distributed across approximately 12 rooftops, each averaging 92 panels, assuming a standard rooftop area of 250m². This configuration optimizes land use, and ensures proximity to load centers, in a space-constraint urban center. However, this distributed topology may introduce potential transmission inefficiencies. Additionally, for the inverter selection, the Sungrow SG80KTL model, a three-phase inverter with a maximum PV array power of 80kW, is used. This inverter supports a maximum DC input voltage of 950V, and an input current of 115A, making it suitable for high-capacity PV systems. The inverter capacity is derived, by applying an oversizing factor of 1.11 [13], to the total DC power output of 598kWp, resulting in an AC-rated capacity of 538.74kWp. To achieve this, the system uses seven inverters, each with a nominal rating of 80kW, providing a cumulative installed capacity of 560kWp. This configuration of 560kWp, taking into consideration energy losses, closely matches with the required power capacity of 538.74kWp, ensuring optimal energy conversion efficiency and maintaining system reliability under operational conditions.

4. Results

There are 56 iterative simulations performed using the PVSyst software tool. These simulations went through repeated computational cycles, to achieve high precision and minimize numerical discrepancies. Critical PV system performance parameters, including the energy output per year, performance ratio (P.R.), and capacity factor (C.F.), are analyzed.

4.1 Photovoltaic (PV) Modelling

The PV modeling includes the following characteristics:

- Analyzing P.R. and C.F. evaluates PV efficiency, degradation and reliability, enabling precise energy output modeling.
- The P.R., which represents the efficiency of converting incident solar irradiance into electrical energy, was 0.8 for mPVs and 0.9 for bPVs on average, across the seven cities, and all tilt configurations. This shows that bPVs exhibit a 10% superior energy conversion efficiency, effectively using both direct solar irradiance and albedo-reflected irradiance, for enhanced PV performance.
- The C.F. represents the ratio of the actual energy output, to the maximum theoretical energy output, based on rated power output. As illustrated in Table 3, the C.F. range for bPVs (13-22%) exceeds that of mPVs (11-20%), on average.
- The optimal tilt angle for maximum energy generation is 30°. The lowest energy output is at a tilt angle of 0°. The reduced energy output at 0° is due to an inefficient incidence angle, limiting irradiance absorption, and increasing Fresnel reflection losses. Also, this orientation results in more dirt and dust building up on the module surface, decreasing active and passive convective cooling efficiency, and increasing module-operating temperatures. This worsens the module temperature conditions and collectively impacts the PV's system's power conversion efficiency and energy output at 0° [8].
- Energy output results for mPVs and bPVs are classified into high, intermediate, and low. Almeria, Seville, and Tenerife exhibit high energy outputs. This is due to the high direct normal irradiance, low diffuse fraction, and elevated ground albedo, enhancing rear-surface bifacial irradiance. The bPVs exhibit a 7-10% higher energy conversion efficiency, as compared to mPVs in these cities.
- Bilbao has the lowest annual energy output for mPVs (600MWh) and bPVs (672MWh) as seen in Table 3. This is due to factors including reduced solar irradiance availability, frequent cloud attenuation, and a high diffuse irradiance ratio, characteristic of northern latitude weather conditions.
- Barcelona, Madrid, and Zaragoza show moderate PV energy generation, which is reflective of their intermediate GHI values, spectral irradiance quality, and elevated atmospheric scattering coefficients.
- A curious observation is that even though Bilbao and Tenerife are both coastal cities, the PV energy outputs contrast. This is due to Tenerife's higher direct normal irradiance and lower diffuse light fraction, compared to Bilbao's frequent cloud cover and high diffuse irradiance ratio. Also, Tenerife competes with Seville and Almería in energy output, because extreme heatwaves in these two cities, during summer, can stress electrical systems and reduce the efficiency of PV panels. These regions often experience temperatures that exceed the optimal operating range for most panels. Tenerife's milder summers allow panels to operate closer to their peak efficiency.

4.2 Pitch, GCR and Limit Angle

One of the cities with the highest energy outputs, is selected to determine if further energy gains can be achieved through adjustments in the PV panel layout characteristics. Almeria, achieving peak energy generation at a 30° tilt (bPV: 1,120 MWh/year), undergoes optimization efforts by modifying key system parameters, such as the shading limiting angle,

ground cover ratio (GCR), and array pitch, as outlined in Table 4.

Table 3. Energy Output and Performance of bPV vs. mPV Systems

DEG	BNA	MAD	SEV	BIL	ZGZ	TFE	ALM
BIFACIAL - Energy Output – per year (MWh/yr.)							
0	870	892	964	672	891	1062	981
15	969	983	1065	732	990	1136	1081
30	1013	1019	1102	756	1032	1147	1120
45	1008	1006	1085	746	1022	1102	1103
CAPACITY FACTOR (C.F)							
0	16.84	17.27	18.67	13.02	17.25	20.61	19.02
15	18.76	19.05	20.61	14.18	19.18	22.06	20.98
30	19.62	19.74	21.33	14.66	20.00	22.29	21.75
45	19.52	19.48	21.02	14.47	19.81	21.44	21.44
MONOFACIAL - Energy Output – per year (MWh/yr.)							
0	779	799	867	600	799	960	881
15	877	891	984	661	898	1031	981
30	926	932	1027	687	946	1043	1025
45	923	921	1014	678	939	997	1010
CAPACITY FACTOR (C.F)							
0	15.07	15.486	16.79	11.64	15.47	18.63	17.08
15	16.99	17.267	19.06	12.82	17.40	20.03	19.05
30	17.94	18.057	19.88	13.34	18.33	20.27	19.90
45	17.87	17.856	19.64	13.16	18.22	19.41	19.64

Table 4. Impact of Shading Angle, GCR, and Pitch on PV Output

Limit Angle (°)	GCR	Pitch (m)	MWh/yr
13.3	0.33	9	1120
14	0.35	8.65	1118
16.2	0.38	7.8	1112
11.6	0.3	10	1125
15.1	0.37	8.2	1115
20.3	0.45	6.7	1099
10.2	0.27	11	1128

As the limit angle increases, energy output tends to decrease due to reduced solar exposure at sharper PV array angles, as seen in Table 4. From Figure 2, it is also observed that a higher pitch improves energy output, by reducing shading and increasing module spacing.

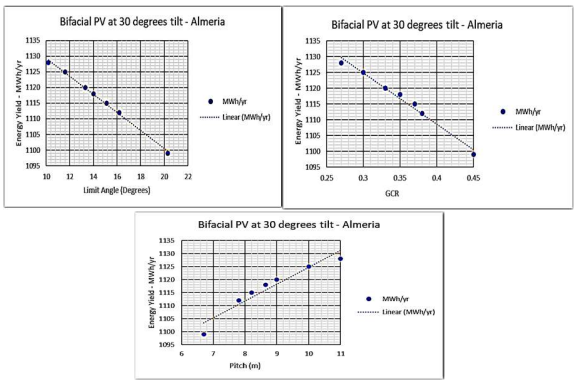

Figure 2. Graph of bPV-MWh/yr. vs. Limit Angle, GCR, and Pitch in Almeria

The optimal GCR maximizes energy capture without excessive land usage, leading to higher energy generation. The highest energy output of 1128MWh/year is achieved with a limit angle of 10.2° and a GCR of 0.27. There is also a pitch of 11m. This shows that minimizing the GCR and limit angle, while maximizing the pitch, optimizes energy capture by reducing shading. This optimization, combined with the integration of battery energy storage systems (BESS), with DCFCS and PV systems, supports 800V EV fast charging.

4.3 PV Energy Storage for 800V Electric Vehicles

The BESS consists of 10 modules connected in series and 21 in parallel, making a total of 210 battery modules. Each module operates at 25.6V and 180Ah, delivering a battery pack voltage of 256V and a global capacity of 3780Ah. This results in 774kWh of stored energy at 80% DoD. European practices, such as those outlined in the European Green Deal and Energy Storage Action Plans, suggest 5–10% storage ratios to support fluctuations from intermittent sources like solar PV [15].

Table 5. Energy Storage and Grid Roles for bPVs and mPVs

PV Type	EV Energy Demand (MWh/day)	EV Energy Demand-800V (MWh/year)	PV Energy to Grid (MWh/year)	Energy From Grid to 800V EV (MWh/year)	% Contribution
Bifacial PV	16.8	6132	1120	5012	18.26
Monofacial PV	16.8	6132	1025	5107	16.72

The 774kWh BESS, as calculated using PVSyst in the paper, represents about 4.6% of the total energy demand of 16,800kWh. This value is slightly approximate to the 5% benchmark, commonly referenced in European energy storage guidelines. The result highlights the system's alignment with standard energy storage practices. With a nominal PV array of 598 kWp, BESS is vital to meet the peak power of 564kWp during peak times of charging. The single-line diagram in Figure 3 illustrates the configuration of bPV arrays, connected through combiners and inverters (160 kVA and 400 kVA) to the grid injection point, enabling efficient energy transfer and further supporting reduced reliance on grid-supplied power. As presented in Table 5, bPVs show a 1.54% decrease in grid dependency, with grid-supplied contribution of 5012MWh/year, as compared to 5107MWh/year for mPV systems. During peak shaving periods, only 0.5% of the energy discharged from the BESS, originates from the PV system (bPVs). Due to the system's city center location, and with high EV demand, grid dependency remains significant, resulting in minimal contribution from the BESS. Generally, bPVs cost 10% to 20% more than mPVs, with an estimated price difference of €0.02 to €0.05 per watt. They offer a 6% to 10% higher energy yield, potentially reducing long-term Levelized Cost of Electricity (LCOE) and improving economic viability in high-albedo environments [14].

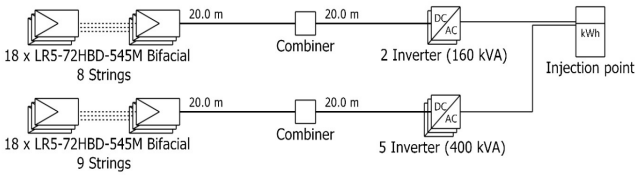

Figure 3. Bifacial PV String and Inverter Configuration for Grid Injection

5. Conclusion

Integrating bPVs, BESS, and DCFCS, effectively support 800V EV fast charging, while reducing grid dependency. In cities with high direct normal irradiance, global horizontal irradiance values, and high PV energy output (Seville, Almeria and Tenerife), the bPVs exhibit a 7-10% higher energy conversion efficiency, as compared to mPVs. The angle, 30º, represents the optimal angle of tilt, for higher PV energy output while 0º is the least desired angle for higher energy output. The bPVs show a 1.54% decrease in grid dependency. Grid-supplied contribution of 5012MWh/year (bPVs), as compared to 5107MWh/year for mPV systems is proven. A further modification of the PV layout, in urban centers (building rooftops), in Almeria, generates 1128MWh/year with a 10.2° limit angle, 0.27 GCR, and 11-meter pitch, optimizing energy capture than initial energy estimates. The 774kWh BESS, representing 4.6% of total energy demand (16,800 kWh), supports peak shaving, but provides only 0.5% of stored energy during peak periods, due to high EV demand and city-center grid reliance. With a nominal PV array of 598kWp and a peak power requirement of 564kWp, the system shows the potential for optimized renewable energy integration and improved grid independence. Further studies could evaluate the impact of tracking systems, such as single-axis horizontal, dual-axis, and vertical tracking, to maximize energy capture and storage potential for both PV types in high-voltage EV applications.

Acknowledgement

The authors thank the Basque Government, GISEL research group (GIC21/180, IT1522-22) and the University of the Basque Country UPV/EHU for their support. The authors declare no conflict of interest.

References

[1] N. Deb and R. Singh, "Journal of Energy and Power Technology An 800V End to End SiC Powertrain to Accommodate Extremely Fast Charging," 2023, doi: 10.21926/jept.2301007.

[2] C. Jung, "Power Up with 800-V Systems," *IEEE Electrif. Mag.*, vol. 5, pp. 53–58, 2017, doi: 10.1109/MELE.2016.2644560.

[3] S. S. G. Acharige, M. E. Haque, M. T. Arif, N. Hosseinzadeh, K. N. Hasan, and A. M. T. Oo, "Review of Electric Vehicle Charging Technologies, Standards, Architectures, and Converter Configurations," *IEEE Access*, vol. 11, pp. 41218–41255, 2023, doi: 10.1109/ACCESS.2023.3267164.

[4] M. A. Mohamed and F. A. Mohamed, "Design and Simulate an Off-Grid PV System with a Battery Bank for EV Charging," *Univers. J. Electr. Electron. Eng.*, vol. 7, no. 5, pp. 273–288, 2020, doi: 10.13189/ujeee.2020.070502.

[5] M. S. Islam, "Analysis of Fast Charging Topologies of Electric Vehicles," Lappeenranta–Lahti University of Technology LUT Master's, 2024.

[6] M. Gjelaj, C. Træholt, S. Hashemi, and P. B. Andersen, "Optimal design of DC fast-charging stations for EVs in low voltage grids," *2017 IEEE Transp. Electrif. Conf. Expo, ITEC 2017*, pp. 684–689, 2017, doi: 10.1109/ITEC.2017.7993352.

[7] E. Muñoz-Cerón, S. Moreno-Buesa, J. Leloux, J. Aguilera, and D. Moser, "Evaluation of the bifaciality coefficient of bifacial photovoltaic modules under real operating conditions," *J. Clean. Prod.*, vol. 434, no. December, 2024, doi: 10.1016/j.jclepro.2023.139807.

[8] E. Türkdoğru and M. Kutay, "Analysis of albedo effect in a 30-kW bifacial PV system with different ground surfaces using PVSYST software," *J. Energy Syst.*, vol. 6, no. 4, pp. 543–559, 2022, doi: 10.30521/jes.1105348.

[9] A. Wallberg, C. Flygare, R. Waters, and V. Castellucci, "Peak Shaving for Electric Vehicle Charging Infrastructure—A Case Study in a Parking Garage in Uppsala, Sweden," *World Electr. Veh. J.*, vol. 13, no. 8, 2022, doi: 10.3390/wevj13080152.

[10] https://www.aemet.es/es/portada, "AEMET," 2024. .

[11] M. Gilleran *et al.*, "Impact of electric vehicle charging on the power demand of retail buildings," *Adv. Appl. Energy*, vol. 4, no. August, p. 100062, 2021, doi: 10.1016/j.adapen.2021.100062.

[12] European Commission, "EU Solar Energy Strategy. Legislative train 12.2024 1," 2024.

[13] M. J. Mayer, "Impact of the tilt angle, inverter sizing factor and row spacing on the photovoltaic power forecast accuracy," *Appl. Energy*, vol. 323, no. June, 2022, doi: 10.1016/j.apenergy.2022.119598.

[14] C. McDevitt and J. Marsh, "Bifacial solar panels: What you need to know," 2024. https://www.energysage.com/solar/bifacial-solar-panels-what-you-need-to-know/.

[15] D. Liu, F. Zhao, S. Wang, Y. Cui, and J. Shu, "Optimal allocation method of energy storage for integrated renewable generation plants based on power market simulation," *Energy Storage Sav.*, vol. 2, no. 3, pp. 540–547, 2023, doi: 10.1016/j.enss.2023.02.007.